LETTERS

Cold streams in early massive hot haloes as the main mode of galaxy formation

A. Dekel[1], Y. Birnboim[1,2], G. Engel[1], J. Freundlich[1,3], T. Goerdt[1], M. Mumcuoglu[1], E. Neistein[1,4], C. Pichon[5], R. Teyssier[6,7] & E. Zinger[1]

Massive galaxies in the young Universe, ten billion years ago, formed stars at surprising intensities[1,2]. Although this is commonly attributed to violent mergers, the properties of many of these galaxies are incompatible with such events, showing gas-rich, clumpy, extended rotating disks not dominated by spheroids[1–5]. Cosmological simulations[6] and clustering theory[6,7] are used to explore how these galaxies acquired their gas. Here we report that they are 'stream-fed galaxies', formed from steady, narrow, cold gas streams that penetrate the shock-heated media of massive dark matter haloes[8,9]. A comparison with the observed abundance of star-forming galaxies implies that most of the input gas must rapidly convert to stars. One-third of the stream mass is in gas clumps leading to mergers of mass ratio greater than 1:10, and the rest is in smoother flows. With a merger duty cycle of 0.1, three-quarters of the galaxies forming stars at a given rate are fed by smooth streams. The rarer, submillimetre galaxies that form stars even more intensely[2,12,13] are largely merger-induced starbursts. Unlike destructive mergers, the streams are likely to keep the rotating disk configuration intact, although turbulent and broken into giant star-forming clumps that merge into a central spheroid[4,10,11]. This stream-driven scenario for the formation of discs and spheroids is an alternative to the merger picture.

It appears that the most effective star formers in the Universe were galaxies of stellar and gas masses of $\sim 10^{11} M_{\odot}$ at redshifts $z = 2-3$, when the Universe was ~3 Gyr old. ($M_{\odot}$, solar mass.) The common cases[1,3] show star-formation rates (SFRs) of $100 M_{\odot} - 200 M_{\odot}\,\mathrm{yr}^{-1}$. These include ultraviolet-selected galaxies termed BX/BM galaxies (ref. 14) and rest-frame optically selected galaxies termed sBzK galaxies (ref. 15), to be referred to collectively as 'star-forming galaxies' (SFGs). Their SFRs are much higher than the $4 M_{\odot}\,\mathrm{yr}^{-1}$ in today's Milky Way, although their masses and dynamical times are comparable. The co-moving space density of SFGs is $n \approx 2 \times 10^{-4}\,\mathrm{Mpc}^{-3}$, implying, within the standard cosmology (termed ΛCDM), that they reside in dark matter haloes of mass $\lesssim 3.5 \times 10^{12} M_{\odot}$. The most extreme star formers are dusty submillimetre galaxies (SMG)[12,13], with SFRs of up to $\sim 1{,}000 M_{\odot}\,\mathrm{yr}^{-1}$ and $n \approx 2 \times 10^{-5}\,\mathrm{Mpc}^{-3}$. Whereas most SMGs could be starbursts induced by major mergers, the kinematics of the SFGs indicate extended, clumpy, thick rotating disks that are incompatible with the expected compact or highly perturbed kinematics of ongoing mergers[1,3,4]. The puzzle is how massive galaxies form most of their stars so efficiently at early times through a process other than a major merger. A necessary condition is a steady, rapid gas supply into massive disks.

It is first necessary to verify that the required rate of gas supply is compatible with the cosmological growth rate of dark matter haloes. The average growth rate of halo mass, M_{v}, through mergers and smooth accretion, is derived[6] on the basis of the extended Press–Schechter (EPS) theory of gravitational clustering (Supplementary Information, section 1) or from cosmological simulations[16,17]. For ΛCDM, the corresponding growth rate of the baryonic component is approximately

$$\dot{M} \approx 6.6 M_{12}^{1.15} (1+z)^{2.25} f_{0.165} M_{\odot}\,\mathrm{yr}^{-1} \quad (1)$$

where $M_{12} \equiv M_{\mathrm{v}}/10^{12} M_{\odot}$ and $f_{0.165}$ is the baryonic fraction in the haloes in units of the cosmological value, $f_{\mathrm{b}} = 0.165$. Thus, at $z = 2.2$, the baryonic growth rate of haloes of mass $2 \times 10^{12} M_{\odot}$ is $\dot{M} \approx 200 M_{\odot}\,\mathrm{yr}^{-1}$, sufficient to maintain the SFR in SFGs. However, the margin by which this is sufficient is not large, implying that (1) the incoming material must be mostly gaseous, (2) the cold gas must efficiently penetrate into the inner halo and (3) the SFR must closely follow the gas supply rate.

The deep penetration is not a trivial matter, given that halo masses of $M_{\mathrm{v}} > 10^{12} M_{\odot}$ are above the threshold for virial shock heating[8,9,18–21], $M_{\mathrm{shock}} \lesssim 10^{12} M_{\odot}$. Such haloes are encompassed by a stable shock near their outer radius, R_{v}, inside which gravity and thermal energy are in virial equilibrium. Gas falling in through the shock is expected to heat up to the virial temperature and stall in quasi-static equilibrium before it cools and descends into the inner galaxy[22]. However, at $z \geq 2$, these hot haloes are penetrated by cold streams[8,9,20]. Because early haloes with $M_{\mathrm{v}} > M_{\mathrm{shock}}$ populate the massive tail of the distribution, they are fed by dark matter filaments from the cosmic web that are narrow in comparison with R_{v} and denser than the mean within the halo[8]. The enhanced density of the gas along these filaments makes the flows along them unstoppable; in particular, they cool before they develop the pressure to support a shock, and thus avoid shock heating (Supplementary Information, section 2).

To investigate the penetration of cold streams, we study the way gas feeds massive high-z galaxies in the cosmological MareNostrum simulation—an adaptive-mesh hydrodynamical simulation in a co-moving box of side length 71 Mpc and a resolution of 1.4 kpc at the galaxy centres (Supplementary Information, section 3). The gas maps in Figs 1 and 2 demonstrate how the shock-heated, high-entropy, low-flux medium that fills most of the halo is penetrated by three narrow, high-flux streams of low-entropy gas (Supplementary Figs 3–6). The penetration is evaluated from the profiles of gas inflow rate, $\dot{M}(r)$, through shells of radius r (Fig. 3, Supplementary Fig. 7). The average profile reveals that the flow rate remains constant from well outside $R_{\mathrm{v}} \approx 90$ kpc to the disk inside $r \approx 15$ kpc.

To relate the feeding by streams to the observed abundance of galaxies as a function of SFR, we use the MareNostrum inflow-rate profiles to evaluate $n(>\dot{M})$, the co-moving number density of galaxies with an inflow rate $>\dot{M}$. We first extract the conditional probability distribution $P(\dot{M} \mid M_{\mathrm{v}})$ by sampling the $\dot{M}(r)$ profiles

[1]Racah Institute of Physics, The Hebrew University, Jerusalem 91904, Israel. [2]Harvard Smithsonian Center for Astrophysics, 60 Garden St, Cambridge, Massachusetts 02138, USA. [3]Departement de Physique, ENS, 24 rue Lhomond, 75231 Paris cedex 05, France. [4]Max Planck Institute for Astrophysics, Karl-Schwarzschild-Strasse 1, 85741 Garching, Germany. [5]Institut d'Astrophysique de Paris and UPMC, 98bis Boulevard Arago, Paris 75014, France. [6]CEA Saclay, DSM/IRFU, UMR AIM, Batiment 709, 91191 Gif-sur-Yvette cedex, France. [7]Institute for Theoretical Physics, University of Zurich, CH-8057 Zurich, Switzerland.

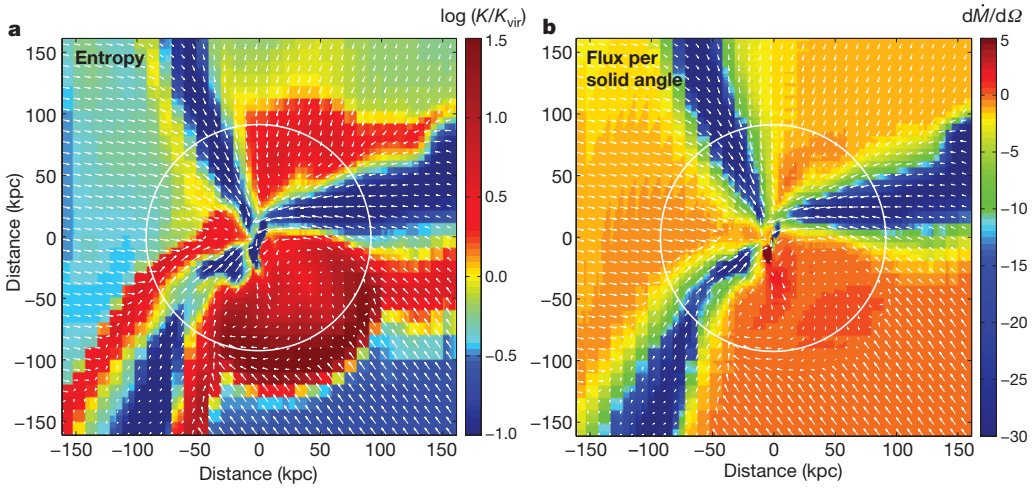

Figure 1 | Entropy, velocity and inward flux of cold streams penetrating hot haloes. **a**, **b**, Maps referring to a thin slice through one of our fiducial galaxies with $M_v = 10^{12} M_\odot$ at $z = 2.5$. The arrows describe the velocity field, scaled such that the distance between the tails is 260 km s^{-1}. The circle marks the halo virial radius, R_v. The entropy, $\log K = \log(T/\rho^{2/3})$, in units of the virial quantities, highlights (in red) the high-entropy medium filling the halo out to the virial shock outside R_v. It exhibits (in blue) three radial, low-entropy streams that penetrate the inner disk, seen edge-on. The radial flux per solid angle is $\dot{m} = r^2 \rho v_r$, in solar masses per year per square radian, where ρ is the gas density and v_r the radial velocity. It demonstrates that more than 90% of the inflow is channelled through the streams (blue), at a rate that remains roughly the same at all radii. This rate is several times higher than the spherical average outside the virial sphere, $\dot{m}_{vir} \approx 8 M_\odot\,\mathrm{yr}^{-1}\,\mathrm{rad}^{-2}$, according to equation (1). The opening angle of a typical stream at R_v is $20^\circ - 30^\circ$, so the streams cover a total angular area of ~ 0.4 rad^2, namely a few per cent of the sphere. When viewed from a given direction, the column density of cold gas below 10^5 K is above 10^{20} cm^{-2} for 25% of the area within the virial radius. Although the pictures show the inner disk, the disk width is not resolved, so associated phenomena such as shocks, star formation and feedback are treated in an approximate way only (see density maps and additional cases in Supplementary Figs 3–5). K_{vir}, virial entropy.

uniformly in r, using the fact that the velocity along the streams is roughly constant (Supplementary Information, sections 5 and 6). This is convolved with the halo mass function[23], $n(M_v)$, to give

$$n(\dot{M}) = \int_0^\infty P(\dot{M}\,|M_v)\, n(M_v)\, \mathrm{d}M_v$$

The desired cumulative abundance, $n(>\dot{M})$, obtained by integration over the inflow rates from $\dot{M}$ to infinity, is shown at $z = 2.2$ in Fig. 4. Assuming that the SFR equals $\dot{M}$, the curve referring to $\dot{M}$ lies safely above the observed values, marked by the symbols, indicating that the gas input rate is sufficient to explain the SFR. However, $\dot{M}$ and the SFR are allowed to differ only by a factor of ~ 2, confirming our suspicion that the SFR must closely follow the gas input rate. The simulated SFR indeed traces the accretion rate to within a factor of two, but, given that our disks are poorly resolved, we focus here on the accretion as the more robustly simulated quantity. Because at $z \approx 2.2$ the star-forming galaxies constitute only a fraction of the observed $\sim 10^{11} M_\odot$ galaxies[24,25], the requirement for a SFR almost as great as $\dot{M}$, based on Fig. 4, becomes even stronger.

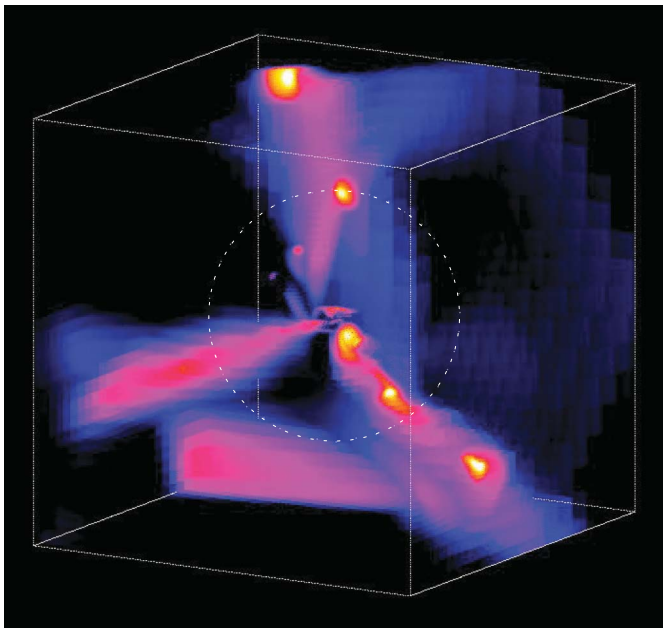

Figure 2 | Streams in three dimensions. The map shows radial flux for the galaxy of Fig. 1 in a box of side length 320 kpc. The colours refer to inflow rate per solid angle of point-like tracers at the centres of cubic-grid cells. The dotted circle marks the halo virial radius. The appearance of three fairly radial streams seems to be generic in massive haloes at high redshift, and is a feature of the cosmic web that deserves an explanation. Two of the streams show gas clumps of mass on the order of one-tenth that of the central galaxy, but most of the stream mass is smoother (Supplementary Fig. 6). The $\gtrsim 10^{10} M_\odot$ clumps, which involve about one-third of the incoming mass, are also gas rich—in the current simulation only 30% of their baryons turn into stars before they merge with the central galaxy.

By analysing the clumpiness of the gas streams, using the sharp peaks of inflow in the $\dot{M}(r)$ profiles, we address the role of mergers versus smooth flows. We evaluate each clump mass by integrating $M_{clump} = \int (\dot{M}(r)/v_r(r))\, \mathrm{d}r$ across the peak, and estimate a mass ratio for the expected merger as $\mu = M_{clump}/f_b M_v$, ignoring further mass loss in the clump on its way in and deviations of the galaxy baryon fraction from f_b. We use 'merger' to describe any major or minor merger with $\mu \geq 0.1$, as distinct from 'smooth' flows, which include 'mini-minor' mergers with $\mu < 0.1$. We find that about one-third of the mass is flowing in as mergers and the rest as smoother flows. However, the central galaxy is fed by a clump with $\mu \geq 0.1$ less than 10% of the time; that is, the duty cycle for mergers is $\eta \lesssim 0.1$. A similar estimate is obtained using EPS merger rates[7] and starburst durations of ~ 50 Myr at $z = 2.5$ from simulations[26] (Supplementary Information, section 5).

From the difference between the two curves of Fig. 4, we learn that only one-quarter of the galaxies with a given $\dot{M}$ are to be seen during a merger. The fact that the SFGs lie well above the merger curve even if the SFR is $\sim \dot{M}$ indicates that in most of them the star formation is driven by smooth streams. Thus, 'SFG' could also stand for 'stream-fed galaxy'. This may explain why these galaxies maintain an

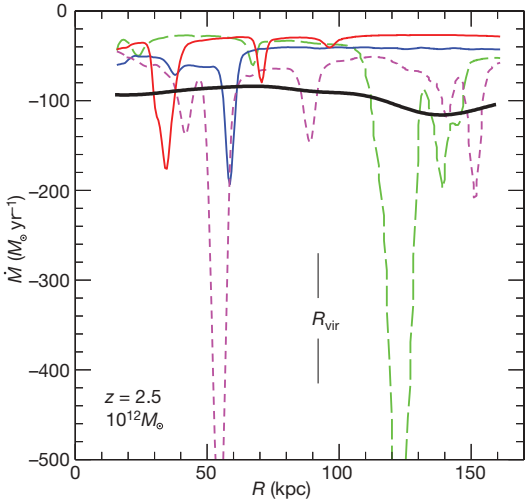

Figure 3 | Accretion profiles, $\dot{M}(r)$. Shown is the gas inflow rate through spherical shells of radius r, from the disk vicinity to almost twice the halo virial radius, obtained by integrating $r^2\rho v_r$ over the whole shell. The thick black curve is the average over the simulated galaxies of the fiducial case, $M_v \approx 10^{12}M_\odot$ at $z = 2.5$. It shows deep penetration at a roughly constant rate of $\sim 100M_\odot$ yr^{-1}, consistent with the virial growth rate predicted by equation (1). Apparently, the inflow rate does decay as the gas travels through the halo, but this decay is roughly compensated for by the higher cosmological inflow rate when that gas entered the halo (equation (1)), leading to the apparent constancy of accretion rate with radius. The coloured curves refer to four representative galaxies, two showing clumps with $\mu \gtrsim 0.1$ (dashed lines) and two with smoother flows involving only mini-minor clumps with $\mu < 0.1$ (solid lines). Clumps with $\mu \gtrsim 0.3$ appear within $2R_v$ about once in every ten galaxies; that is, major mergers are infrequent (Supplementary Fig. 7). The $\dot{M}(r)$ profiles serve for extracting the conditional probability distribution $P(\dot{M} \mid M_v)$, leading to the abundance $n(>\dot{M})$ (Supplementary Fig. 8).

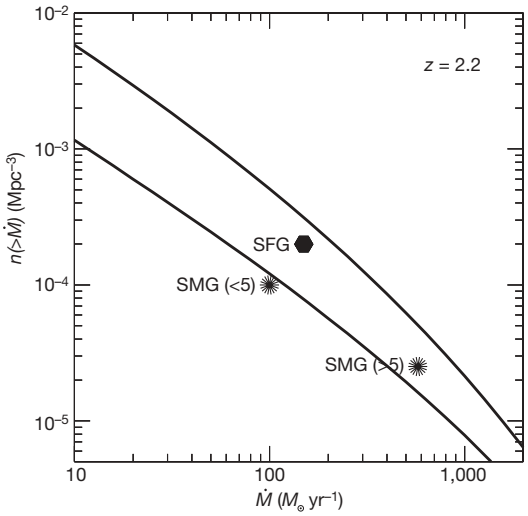

Figure 4 | Abundance of galaxies as a function of gas inflow rate, $n(>\dot{M})$. Shown is the co-moving number density, n, of galaxies with inflow rate higher than $\dot{M}$ at $z = 2.2$, as predicted from our analysis of the cosmological simulation. The upper curve refers to total inflow. It shows that galaxies with $\dot{M} > 150M_\odot$ yr^{-1} are expected at a co-moving number density $n \approx 3 \times 10^{-4}$ Mpc^{-3} (similar to estimates in other simulations[32,33]). Fluxes as high as $\dot{M} > 500M_\odot$ yr^{-1} are anticipated at $n \approx 6 \times 10^{-5}$ Mpc^{-3}. The lower curve is similar, but limited to gas input by $\mu > 0.1$ mergers. The symbols represent the vicinity of where the observed massive star-forming galaxies can be located once their observed SFRs are identified with $\dot{M}$. The sBzK and BX/BM galaxies are marked SFG[13]. The SMGs respectively brighter and fainter than 5 mJy are marked accordingly[12,13]. We see that the overall gas inflow rate is sufficient for the observed SFR, but the small margin implies that the SFR must closely follow the rate of gas supply. Most of the massive star formers at a given SFR are expected to be observed while being fed by smooth flows rather than undergoing mergers. By studying the contribution of different halo masses to the abundance $n(>\dot{M})$, we learn that the high-SFR SFGs and SMGs are associated with haloes of mass $10^{12}M_\odot - 10^{13}M_\odot$ (Supplementary Fig. 9). An integration of $\dot{M}$ over halo mass and time reveals that most of the stars in the universe were formed in stream-fed galaxies, within haloes of mass $>2 \times 10^{11}M_\odot$ at $1.5 < z < 4$.

extended, thick disk while doubling their mass over a halo crossing time[4]. On the other hand, if the SFR is $\sim\dot{M}$, we learn from Fig. 4 that about half of the bright SMGs and most of the fainter SMGs lie below the merger curve and are therefore consistent with being merger-induced starbursts[13].

We find that stream-fed galaxies of mass $\sim 10^{11}M_\odot$ at $z \approx 2.5$ were the most productive star formers in the universe. The constraints on the overall SFR density at these epochs imply that SFR has been suppressed in smaller galaxies, for example by photo-ionization and stellar feedback[8,27,28]. The early presence of low-SFR galaxies[24,25] requires quenching of SFR also at the massive end, perhaps due to gravitational heating by destructive streams[29].

The streams are likely also to be responsible for compact spheroids, as an alternative to mergers and the associated heating by expanding shocks[22,29]. Using equation (1), we find that at $z \geq 2$ the streams can maintain both the high gas fraction and the turbulence necessary for the disk to break up into giant clumps by gravitational instability, with dispersion-to-rotation ratio $\sigma/V \approx 0.25$, as observed[4,30]. The clumps migrate inward and dissipatively merge into a spheroid[10,11]. The stream carrying the largest coherent flux with an impact parameter of a few kiloparsecs determines the disk's spin and orientation, and the stream clumps perturb it. The incoming clumps and the growing spheroid can eventually stabilize the disk and suppress star formation. We can thus associate the streams with the main mode of galaxy and star formation occurring in massive haloes at $z \approx 2-3$; the streams that create the disks also make them fragment into giant clumps that serve both as the sites of efficient star formation and the progenitors of the central spheroid, which in turn helps the streams to quench star formation.

Although wet mergers may grow secondary disks[31], they are not as frequent as the observed SFGs (Fig. 4), these disks are neither gas rich nor clumpy enough, and, unlike most SFGs, they are dominated by stellar spheroids.

The cold streams should be detectable by absorption or emission. For external background sources, our simulation predicts that haloes with $M_v \approx 10^{12}M_\odot$ at $z \approx 2.5$ should contain gas at temperature $<10^5$ K with column densities $>10^{20}$ cm^{-2} covering $\sim$25% of the area at radii between 20 and 100 kpc, with coherent velocities of $\lesssim 200$ km s^{-1}. Sources at the central galaxies should show absorption by the radial streams in $\sim$5% of the galaxies, flowing in at $\gtrsim 200$ km s^{-1}, with column densities $\sim 10^{21}$ cm^{-2} (Supplementary Figs 3–5).

Received 30 July; accepted 7 November 2008.

1. Genzel, R. *et al.* The rapid formation of a large rotating disk galaxy three billion years after the Big Bang. *Nature* **442**, 786–789 (2006).
2. Chapman, S. C., Smail, I., Blain, A. W. & Ivison, R. J. A population of hot, dusty ultraluminous galaxies at $z \sim 2$. *Astrophys. J.* **614**, 671–678 (2004).
3. Förster Schreiber, N. M. *et al.* SINFONI integral field spectroscopy of $z \sim 2$ UV-selected galaxies: Rotation curves and dynamical evolution. *Astrophys. J.* **645**, 1062–1075 (2006).
4. Genzel, R. *et al.* From rings to bulges: evidence for rapid secular galaxy evolution at $z \sim 2$ from integral field spectroscopy in the SINS survey. *Astrophys. J.* **687**, 59–77 (2008).
5. Stark, D. P. *et al.* The formation and assembly of a typical star-forming galaxy at $z \approx 3$. *Nature* **455**, 775–777 (2008).
6. Neistein, E., van den Bosch, F. C. & Dekel, A. Natural downsizing in hierarchical galaxy formation. *Mon. Not. R. Astron. Soc.* **372**, 933–948 (2006).
7. Neistein, E. & Dekel, A. Merger rates of dark-matter haloes. *Mon. Not. R. Astron. Soc.* **388**, 1792–1802 (2008).
8. Dekel, A. & Birnboim, Y. Galaxy bimodality due to cold flows and shock heating. *Mon. Not. R. Astron. Soc.* **368**, 2–20 (2006).

9. Kereš, D., Katz, N., Weinberg, D. H. & Davé, R. How do galaxies get their gas? *Mon. Not. R. Astron. Soc.* **363,** 2–28 (2005).
10. Noguchi, M. Early evolution of disk galaxies: Formation of bulges in clumpy young galactic disks. *Astrophys. J.* **514,** 77–95 (1999).
11. Elmegreen, B., Bournaud, F. & Elmegreen, D. M. Bulge formation by the coalescence of giant clumps in primordial disk galaxies. *Astrophys. J.* **688,** 67–77 (2008).
12. Wall, J. V., Pope, A. & Scott, D. The evolution of submillimetre galaxies: two populations and a redshift cut-off. *Mon. Not. R. Astron. Soc.* **383,** 435–444 (2008).
13. Tacconi, L. J. *et al.* Submillimeter galaxies at $z \sim 2$: Evidence for major mergers and constraints on lifetimes, IMF, and CO-H_2 conversion factor. *Astrophys. J.* **680,** 246–262 (2008).
14. Adelberger, K. L. *et al.* Optical selection of star-forming galaxies at redshifts $1 < z$ 3. *Astrophys. J.* **607,** 226–240 (2004).
15. Daddi, E. *et al.* A new photometric technique for the joint selection of star-forming and passive galaxies at $1.4 < z$ 2.5. *Astrophys. J.* **617,** 746–764 (2004).
16. Neistein, E. & Dekel, A. Constructing merger trees that mimic N-body simulations. *Mon. Not. R. Astron. Soc.* **383,** 615–626 (2008).
17. Genel, S. *et al.* Mergers and mass accretion rates in galaxy assembly: The millennium simulation compared to observations of $z \sim 2$ galaxies. *Astrophys. J.* **688,** 789–793 (2008).
18. Birnboim, Y. & Dekel, A. Virial shocks in galactic haloes? *Mon. Not. R. Astron. Soc.* **345,** 349–364 (2003).
19. Binney, J. On the origin of the galaxy luminosity function. *Mon. Not. R. Astron. Soc.* **347,** 1093–1096 (2004).
20. Ocvirk, P., Pichon, C. & Teyssier, R. Bimodal gas accretion in the MareNostrum galaxy formation simulation. *Mon. Not. R. Astron. Soc.* **390,** 1326–1338 (2008).
21. Keres, D. *et al.* Galaxies in a simulated ΛCDM Universe I: cold mode and hot cores. Preprint at ⟨http://arxiv.org/abs/0809.1430⟩ (2008).
22. Birnboim, Y., Dekel, A. & Neistein, E. Bursting and quenching in massive galaxies without major mergers or AGNs. *Mon. Not. R. Astron. Soc.* **380,** 339–352 (2007).
23. Sheth, R. K. & Tormen, G. An excursion set model of hierarchical clustering: ellipsoidal collapse and the moving barrier. *Mon. Not. R. Astron. Soc.* **329,** 61–75 (2002).
24. Kriek, M. *et al.* Spectroscopic identification of massive galaxies at $z \sim 2.3$ with strongly suppressed star formation. *Astrophys. J.* **649,** L71–L74 (2006).
25. van Dokkum, P. G. *et al.* Confirmation of the remarkable compactness of massive quiescent galaxies at $z \sim 2.3$: Early-type galaxies did not form in a simple monolithic collapse. *Astrophys. J.* **677,** L5–L8 (2008).
26. Cox, T. J., Jonsson, P., Somerville, R. S., Primack, J. R. & Dekel, A. The effect of galaxy mass ratio on merger-driven starbursts. *Mon. Not. R. Astron. Soc.* **384,** 386–409 (2008).
27. Dekel, A. & Silk, J. The origin of dwarf galaxies, cold dark matter, and biased galaxy formation. *Astrophys. J.* **303,** 39–55 (1986).
28. Dekel, A. & Woo, J. Feedback and the fundamental line of low-luminosity low-surface-brightness/dwarf galaxies. *Mon. Not. R. Astron. Soc.* **344,** 1131–1144 (2003).
29. Dekel, A. & Birnboim, Y. Gravitational quenching in massive galaxies and clusters by clumpy accretion. *Mon. Not. R. Astron. Soc.* **383,** 119–138 (2008).
30. Elmegreen, D. M., Elmegreen, B. G. & Hirst, A. C. Discovery of face-on counterparts of chain galaxies in the Tadpole Advanced Camera for Surveys Field. *Astrophys. J.* **604,** L21–L23 (2004).
31. Robertson, B. E. & Bullock, J. S. High-redshift galaxy kinematics: Constraints on models of disk formation. *Astrophys. J.* **685,** L27–L30 (2004).
32. Finlator, K., Davé, R., Papovich, C. & Hernquist, L. The physical and photometric properties of high-redshift galaxies in cosmological hydrodynamic simulations. *Astrophys. J.* **639,** 672–694 (2006).
33. Nagamine, K., Ouchi, M., Springel, V. & Hernquist, L. Lyman-alpha emitters and Lyman-break galaxies at $z = 3$–6 in cosmological SPH simulations. Preprint at ⟨http://arxiv.org/abs/0802.0228⟩ (2008).

Supplementary Information is linked to the online version of the paper at www.nature.com/nature.

Acknowledgements We acknowledge discussions with N. Bouche, S. M. Faber, R. Genzel, D. Koo, A. Kravtsov, A. Pope, J. R. Primack, J. Prochaska, A. Sternberg and J. Wall. This research was supported by the France–Israel Teamwork in Sciences, the German–Israel Science Foundation, the Israel Science Foundation, a NASA Theory Program at UCSC, and a Minerva fellowship (T.G.). We thank the Barcelona Centro Nacional de Supercomputación for computer resources and technical support. The simulation is part of the Horizon collaboration.

Author Information Reprints and permissions information is available at www.nature.com/reprints. Correspondence and requests for materials should be addressed to A.D. (dekel@phys.huji.ac.il).